

AKT signaling restrains tumor suppressive functions of FOXO transcription factors and GSK3 kinase in multiple myeloma

Timon A. Bloedjes,¹ Guus de Wilde,¹ Chiel Maas,¹ Eric Eldering,² Richard J. Bende,¹ Carel J. M. van Noesel,¹ Steven T. Pals,¹ Marcel Spaargaren,¹ and Jeroen E. J. Guikema¹

¹Department of Pathology and ²Department of Experimental Immunology, Amsterdam UMC, University of Amsterdam, Lymphoma and Myeloma Center Amsterdam (LYMMCARE), Amsterdam, The Netherlands

Key Points

- FOXO transcription factors and the GSK3 kinase are pivotal tumor suppressors restrained by AKT activity in MM cells.
- FOXO and GSK3 destabilize MCL1 protein in MM cells.

The phosphatidylinositol-3 kinases and the downstream mediator AKT drive survival and proliferation of multiple myeloma (MM) cells. AKT signaling is active in MM and has pleiotropic effects; however, the key molecular aspects of AKT dependency in MM are not fully clear. Among the various downstream AKT targets are the Forkhead box O (FOXO) transcription factors (TFs) and glycogen synthase kinase 3 (GSK3), which are negatively regulated by AKT signaling. Here we show that abrogation of AKT signaling in MM cells provokes cell death and cell cycle arrest, which crucially depends on both FOXO TFs and GSK3. Based on gene expression profiling, we defined a FOXO-repressed gene set that has prognostic significance in a large cohort of patients with MM, indicating that AKT-mediated gene activation is associated with inferior overall survival. We further show that AKT signaling stabilizes the antiapoptotic myeloid cell leukemia 1 (MCL1) protein by inhibiting FOXO- and GSK3-mediated MCL1 turnover. In concordance, abrogation of AKT signaling greatly sensitized MM cells for an MCL1-targeting BH3-mimetic, which is currently in clinical development. Taken together, our results indicate that AKT activity is required to restrain the tumor-suppressive functions of FOXO and GSK3, thereby stabilizing the antiapoptotic protein MCL1 in MM. These novel insights into the role of AKT in MM pathogenesis and MCL1 regulation provide opportunities to improve targeted therapy for patients with MM.

Introduction

Multiple myeloma (MM) is a malignancy of transformed clonal plasma cells that typically reside in the bone marrow. Despite considerable improvements in the median survival due to new treatment modalities, patients inevitably relapse and become refractory to additional treatment. Further understanding of MM and plasma cell biology is urgently needed and may lead to novel therapeutic strategies.¹

The serine/threonine kinase AKT is a central node in the phosphatidylinositol-3 kinase (PI3K)/AKT/mammalian target of rapamycin (mTOR) pathway, which is active in MM due to growth factors produced by the bone marrow microenvironment, or MM cells.²⁻⁵ Furthermore, hemizygous deletions of phosphatase and tensin homolog, a negative regulator of AKT, were reported in 5% to 20% of MM patients and human myeloma cell lines (HMCL).^{6,7} AKT signaling is involved in cell proliferation, survival, and metabolism.^{3,8} As such, it drives proliferation and sustains the increased energy requirement of MM

Submitted 6 January 2020; accepted 27 July 2020; published online 4 September 2020. DOI 10.1182/bloodadvances.2019001393.

Gene expression profiling data reported in this article have been deposited in the NCBI Gene Expression Omnibus database (accession number GSE120941).

The full-text version of this article contains a data supplement.
© 2020 by The American Society of Hematology

cells by reprogramming various metabolic pathways.⁸ Despite these insights, the downstream effectors that determine the dependence on AKT signaling in MM cells remain largely unexplored.

AKT has many substrates and pleiotropic effects in healthy and malignant cells. In addition to metabolic, translational, and mitogen-activated protein kinase pathways,⁸ forkhead box O transcription factors (FOXOs) and glycogen synthase kinase 3 (GSK3) are negatively regulated by AKT through phosphorylation.⁸ The FOXOs (ie, FOXO1, FOXO3, FOXO4, FOXO6) are context-dependent transcription factors that act as tumor suppressors but may also contribute to tumorigenesis.⁹ Moreover, FOXO1 and FOXO3 have crucial and nonredundant functions in B-cell development, activation, and differentiation.¹⁰⁻¹⁶ FOXOs can be phosphorylated, acetylated, and ubiquitinated by a wide range of enzymes, thereby regulating their stability, localization, and activity.¹⁷ Different interaction partners can also influence the specificity by which FOXO targets genes, regulating their expression.¹⁸ AKT phosphorylates GSK3 on Ser9 (β -isoform) and Ser21 (α -isoform), thereby inhibiting kinase activity.¹⁹⁻²¹ GSK3 is a major AKT target involved in the regulation of cell death by controlling BCL2-family proteins.^{8,22-25} Here, we show that FOXO1/3 and GSK3 are AKT-restrained tumor suppressors and that the expression of FOXO-repressed genes, indicative of increased AKT activity, has prognostic value in a cohort of patients with MM. Mechanistically, we provide evidence that FOXO and GSK3 provoke cell death in a nonredundant fashion through negative regulation of MCL1, a major antiapoptotic protein in plasma cells and MM.²⁵⁻²⁷ In accordance, abrogation of AKT signaling greatly sensitized MM cells for the MCL1 BH3-mimetic S63845, even in MM cells that do not depend on AKT signaling for survival.

Our results clearly show that inactivation of FOXO1/3 and GSK by AKT inhibits their tumor-suppressive functions in MM and, as such, provides a clear rationale to explore therapies aimed at the activation of FOXO and GSK3 combined with inhibition of their downstream targets such as MCL1.

Materials and methods

Cell culture and reagents

The HMCLs LME-1, MM1.S, XG-1, XG-3, LP-1, OPM-2, ANBL-6, UM-3, and RPMI-8226 were cultured in Iscove modified Dulbecco medium (Invitrogen Life Technologies, Carlsbad, CA) supplemented with 2 mM of L-glutamine, 100 U/mL of penicillin, 100 μ g/mL of streptomycin (Gibco, Thermo Fisher Scientific, Waltham, MA), and 10% fetal calf serum (FCS; HyClone, GE Healthcare Life Sciences, Pittsburgh, PA). The cell lines XG-1, XG-3, and ANBL-6 were cultured in medium supplemented with 1 ng/mL interleukin-6 (Prospec Inc., Rehovot, Israel), which was washed out before the experiments. Cytogenetic characteristics, phosphatase and tensin homolog, and TP53 status of these HMCLs can be found in supplemental Table 1. HEK293T cells were obtained from ATCC (Manassas, VA) and cultured in supplemented Dulbecco's modified eagle medium (Invitrogen Life Technologies) and 10% FCS. The following small-molecule inhibitors were used: GSK2110813 (afuresertib) (AKT inhibitor; Selleck Chemicals, Houston, TX), MK2206 (AKT inhibitor; Selleck Chemicals), CHIR99021 (GSK3 inhibitor; Sigma Aldrich, St. Louis, MO), AS1842856 (FOXO1 inhibitor; Merck, Darmstadt, Germany), S63845 (MCL1 inhibitor; Selleck Chemicals), and cycloheximide (Sigma Aldrich).

Constructs and retroviral/lentiviral transductions

CRISPR/Cas9 knockout HMCL clones were generated by lentiviral transduction, as previously described.²⁸ HMCLs overexpressing MCL1 were generated by retroviral transduction using the LZRS-MCL1-IRES-GFP plasmid. A more detailed description is available in the supplemental Materials and methods.

Patient samples

Primary tumor cells from patients with MM (>80% plasma cells) were enriched by Ficoll-Paque PLUS (Cytiva Life Sciences) density centrifugation. Patient material was obtained according to the ethical standards of our institutional medical ethical committee, as well as in agreement with the 1975 Declaration of Helsinki as revised in 1983. Primary MM cells were cultured overnight (16-20 hours) in Iscove modified Dulbecco medium + 10% FCS, supplemented with 1 ng/mL interleukin-6 before being used in further experiments.

Immunoblotting

Immunoblotting experiments were performed as previously described.²⁹ Protocols and antibodies used are available in the supplemental Materials and methods; densitometry quantification of immunoblots was performed by using Image J software (imagej.net).³⁰

Gene expression profiling

RNA from 2×10^6 cells was isolated by using TRI Reagent (Sigma Aldrich) and purified by using the RNeasy Mini Kit (Qiagen, Hilden, Germany) using the RNA cleanup protocol supplied by the manufacturer. The RNA was analyzed by using Affymetrix Human Genome U133 Plus 2.0 arrays (Affymetrix, Santa Clara, CA) and normalized by using MAS5.0 (accession no. GSE120941). Gene expression data were analyzed by using the R2: Genomics Analysis and Visualization Platform (<http://r2.amc.nl>). Venn diagrams were prepared by using BioVenn (www.biovenn.nl).³¹ Enrichment plots were generated by using the Broad Institute Gene Set Enrichment Analysis (GSEA) computational method and software.³²

Flow cytometry

Specific cell death was assessed by 7-aminoactinomycin-D (7-AAD; BioLegend, San Diego, CA) staining and flow cytometry and calculated as reported earlier.³³ Cell cycle analysis was performed by determining DNA content and bromodeoxyuridine incorporation as described previously.²⁸ A detailed protocol is provided in the supplemental Materials and methods.

Statistics

Statistical analysis was performed by using GraphPad Prism software package (GraphPad Software, La Jolla, CA), and combination indexes were calculated by using CompuSyn (CompuSyn Inc., Paramus, NJ).³⁴ In case single-dose drug combinations were used, we calculated the expected effect of drug combinations (C) using the Bliss independence model [$C = A + B - (A*B)$], in which A and B indicate the observed cell death at specific concentrations of the single drugs.³⁵

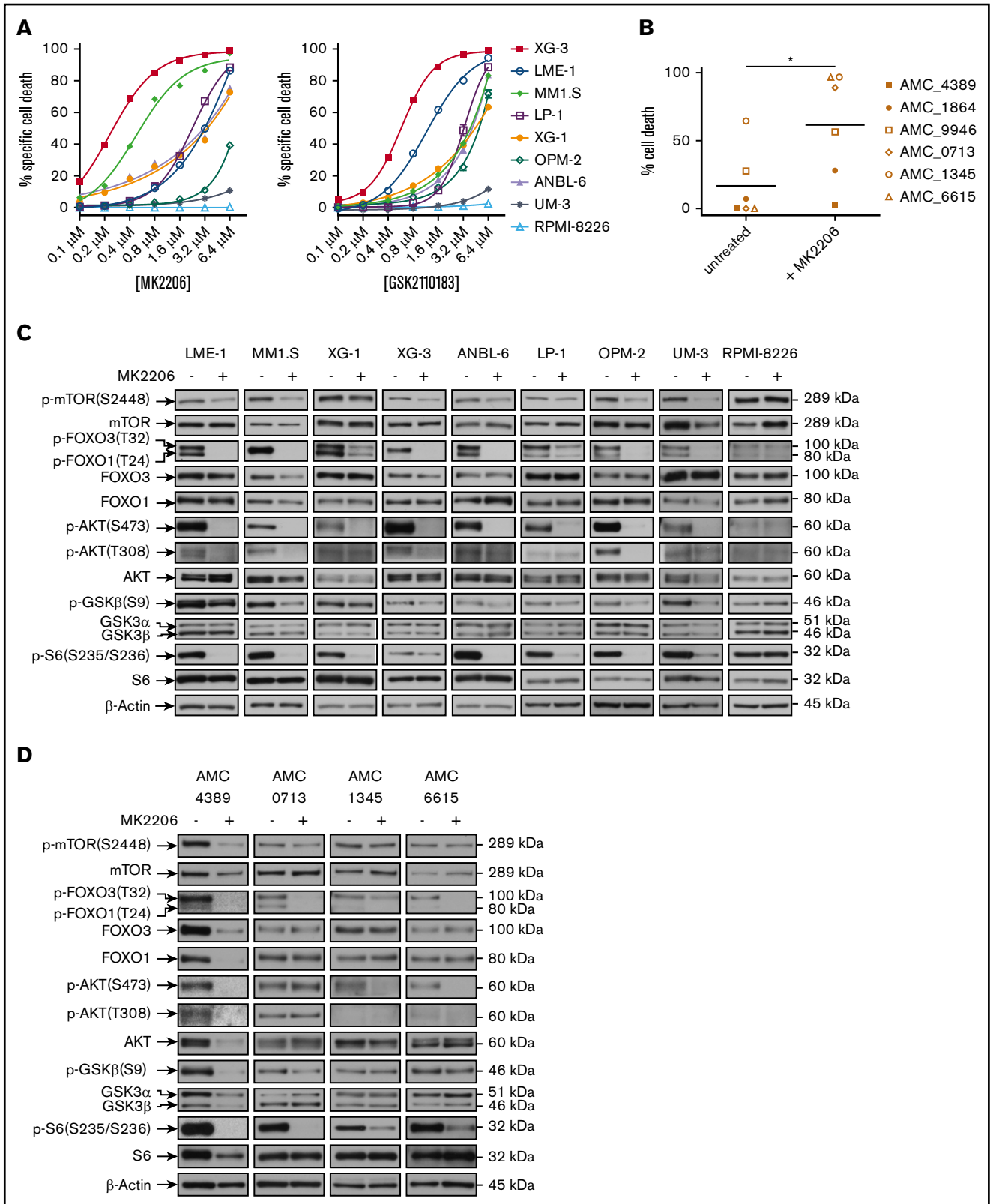


Figure 1. AKT signaling is required for the survival of MM cells. (A) Percentage of specific cell death of HMCLs (n = 9) treated with increasing concentrations of the adenosine triphosphate–competitive AKT inhibitor GSK2110183 (afuresertib) (left panel) and the allosteric AKT inhibitor MK2206 (right panel) for 3 days. Specific cell death was calculated based on 7-AAD viability dye staining and flow cytometry. Mean values of 3 independent experiments are shown. (B) Percentage of cell death of primary MM plasma cells from patients (n = 6) treated with 2.5 μ M MK2206 AKT inhibitor for 3 days. Specific cell death was calculated based on 7-AAD viability dye staining and flow

Results

Prosurvival signaling of AKT in MM cell lines and patient samples

To investigate the AKT signaling cascade in MM, we exposed HMCLs ($n = 9$) to increasing concentrations of the allosteric AKT inhibitor MK2206 or the adenosine triphosphate-competitive AKT inhibitor GSK2110183 (afuresertib), both pan-AKT (AKT1/2/3) inhibitors. AKT signaling is required for the survival of most HMCLs, as both AKT inhibitors potently induced cell death in the majority of the HMCLs. However, UM-3 and RPMI-8226 were refractory to AKT inhibitor-induced cell death (Figure 1A; supplemental Figure 1A-B), indicating that these cell lines do not rely on AKT signaling for survival. Enriched malignant plasma cells obtained from patients with MM ($n = 6$) (supplemental Figure 1C) showed a similar response, in which MK2206 induced cell death to a variable degree in all but 1 patient (Figure 1B).

To assess the downstream effectors of AKT signaling, we performed immunoblotting for several established AKT targets. In all HMCLs except RPMI-8226, inhibition of AKT signaling decreased phosphorylation of AKT Thr308 and Ser473, targets of protein kinase PDK1 and mTOR complex 2 (mTORC2), respectively, that regulate AKT kinase activity.⁸ Moreover, the loss of ribosomal protein S6 phosphorylation, an established AKT substrate, indicated effective inhibition of AKT signaling in all HMCLs except RPMI-8226. Phosphorylation of FOXO1, FOXO3 transcription factors (TFs), and GSK3 β kinase was dependent AKT kinase activity (Figure 1C). In agreement, similar effects of AKT inhibition were observed in primary MM patient samples (Figure 1D).

These results confirm that FOXO and GSK3 are actively suppressed by AKT signaling in HMCLs and primary MM cells.

Activation of FOXO transcription factors induce cell death of MM cells

To assess the involvement of FOXO TFs in prosurvival AKT signaling in MM cells, we generated several FOXO1- and FOXO3-knockout clones for LME-1 ($n = 2$), MM1.S ($n = 4$), and XG-3 ($n = 4$) using CRISPR/Cas9. Loss of FOXO protein expression was confirmed by immunoblotting (Figure 2A). The loss of FOXO had no apparent effect on MM cell survival under basal conditions (supplemental Figure 2A). However, cell death induced by inhibition of AKT kinase activity was rescued by the specific loss of FOXO1 in LME-1 cells, whereas loss of FOXO3 displayed a more partial, although significant, effect on cell death (Figure 2B; supplemental Figure 2B). In contrast, loss of FOXO3 rescued cell death in MM1.S and XG-3 cells, whereas FOXO1 deficiency had no effect on cell death induced by the inhibition of AKT kinase activity in these cell lines. Of interest, we observed a slight increase in FOXO3 protein expression in FOXO1-deficient LME-1 cells and a substantial increase in FOXO1 expression in FOXO3-deficient XG-3 cells.

We confirmed the tumor-suppressive function of FOXO in MM using AS1842856, a small-molecule inhibitor that blocks the transcriptional activity of FOXO1 and, to a far lesser extent, that of FOXO3.³⁶ Similarly to results observed in the FOXO-deficient cells, AS1842856 restored viability of LME-1 cells upon inhibition of AKT kinase activity, whereas it had almost no effect on the induced cell death in MM1.S cells. In other HMCLs, AS1842856 varyingly rescued MK2206-induced cell death (Figure 2C). These results were confirmed in MM patient samples, in which AS1842856 significantly inhibited MK2206-induced cell death in 4 of 5 patient samples tested (Figure 2D). The varying degree of rescue from cell death by AS1842856 may reflect the differential dependency on FOXO1 vs FOXO3 in these patients. Similarly, AS1842856 had no additional effect on FOXO1-deficient LME-1 cells, whereas cell death caused by abrogation of AKT signaling in MM1.S cells, which required FOXO3, was partially rescued by AS1842856 (supplemental Figure 2C). These results clearly show that prosurvival signaling of AKT kinase crucially depends on its inhibitory effect on FOXO TFs, indicating that FOXO TFs are AKT-restrained tumor suppressors in MM.

AKT signaling controls FOXO-dependent gene transcription and repression in MM cells

To determine FOXO-dependent transcriptional changes, we performed gene expression profiling (GEP) of 2 independently established FOXO1-knockout clones from the LME-1 HMCL, and of two FOXO3-knockout clones from the MM1.S and XG-3 HMCLs, respectively. Cloned wild-type “Cas9 only” cells (WT) were used as controls. We anticipated that the 3 HMCLs would exhibit considerable variance in the expression of FOXO target genes, due to the heterogeneous genetic backgrounds of these HMCLs. However, GSEA on the combined GEP datasets clearly indicated significant enrichment of a FOXO3 target gene set in the AKT inhibitor-treated WT control clones (‘WTMK’; WT clones, MK2206-treated) vs the untreated control and FOXO-knockout clones, and AKT inhibitor-treated FOXO-knockout clones (‘REST’) (Figure 3A).

FOXO-regulated genes were identified in MM1.S (848 up, 1541 down), XG-3 (329 up, 382 down), and LME-1 (438 up, 457 down) (Figure 3B; supplemental Table 2). In agreement, *k*-means unsupervised learning and principal component analysis for MM1.S and XG-3 showed that the MK2206-treated control clones (‘WTMK’) consistently clustered together vs a cluster consisting of the untreated control and FOXO3-knockout clones, and the MK2206-treated FOXO3-knockout clones (‘REST’). In contrast, the MK2206-treated control and FOXO1-deficient clones clustered together vs the untreated clones in LME-1. This may reflect intrinsic differences between LME-1 vs MM1.S and XG-3, and/or may indicate that FOXO1 has a less pronounced effect on gene expression compared with FOXO3 (supplemental Figure 3). Comparing these datasets, 23 genes were found to be consistently upregulated and 44 genes were downregulated upon AKT inhibition in a FOXO-dependent fashion (Figure 3B), among which are the

Figure 1. (continued) cytometry. Means of 3 technical replicates are displayed (Wilcoxon signed-rank test, $*P < .05$). (C) Immunoblot analysis of protein expression in AKT-inhibitor treated HMCLs LME-1, MM1.S, XG-1, XG-3, ANBL-6, LP-1, OPM-2, UM-3, and RPMI-8226. Cells were serum starved for 1 hour, after which they were incubated in medium containing 10% FCS with or without 2.5 μ M MK2206 for 2 hours. Shown are the indicated proteins; β -actin was used as a loading control. Representative immunoblot of at least 2 independent experiments is shown. (D) Immunoblot analysis of protein expression in primary MM patient plasma cells ($n = 4$) serum starved for 1 hour, after which they were incubated in medium containing 10% FCS with or without 2.5 μ M MK2206 for 2 hours. Shown are the indicated proteins; β -actin was used as a loading control.

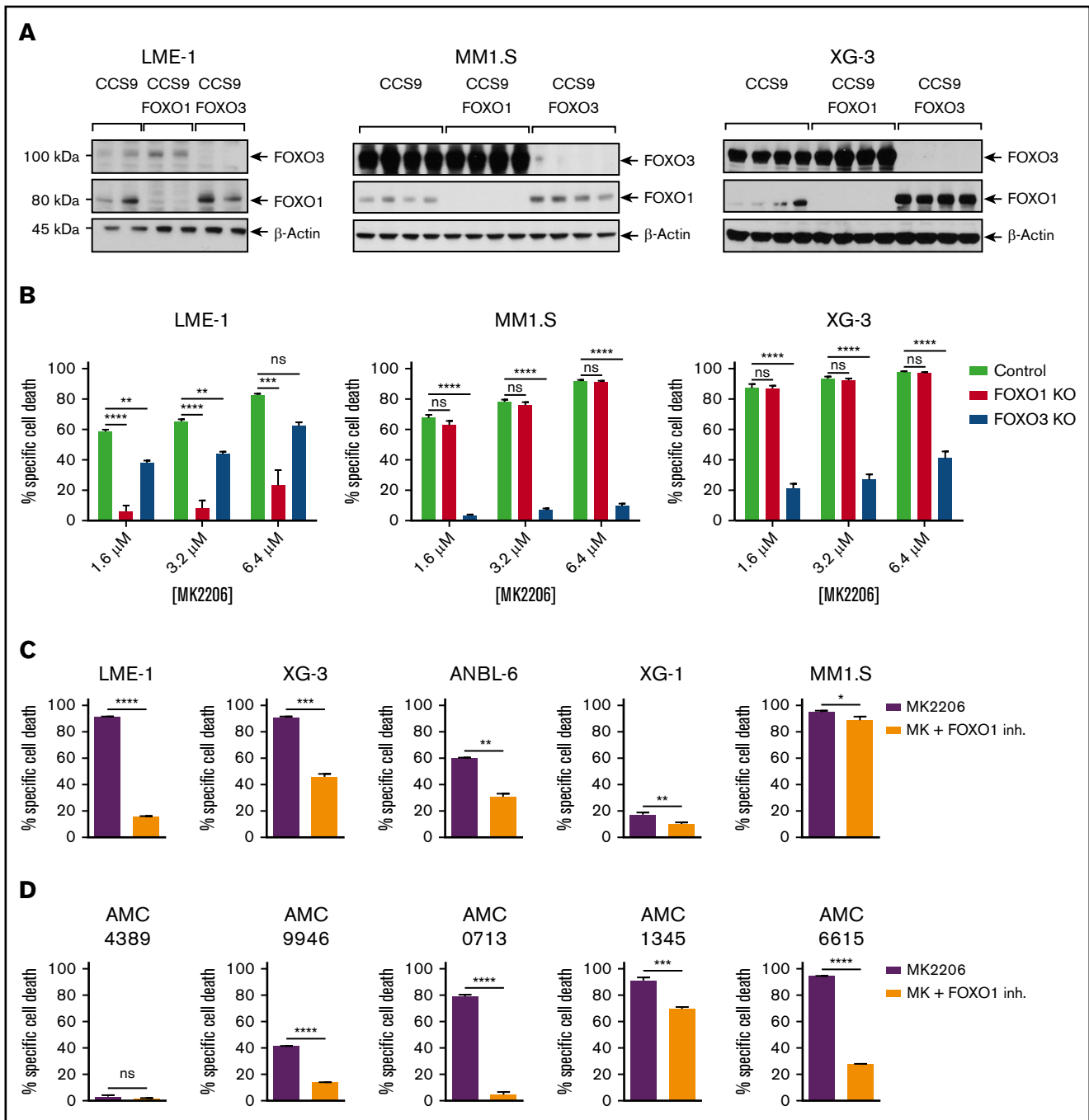


Figure 2. AKT prevents FOXO1- or FOXO3-induced cell death of MM cells. (A) Immunoblot analysis of CRISPR/Cas9-generated FOXO1 and FOXO3 knockout clones of the LME-1 ($n = 2$), MM1.S ($n = 4$), and XG-3 ($n = 4$) HMCLs. β -actin was used as loading control. (B) AKT inhibitor-induced cell death is dependent on the presence of FOXO1 in LME-1 and on FOXO3 in MM1.S and XG-3. Cloned knockout and control HMCLs were treated for 3 days with various concentrations of the MK2206 AKT inhibitor. Two to 4 independently established clones were analyzed per condition. Red bars depict FOXO1 knockout clones; blue bars depict FOXO3 knockout clones. Mean \pm standard error of the mean (SEM) of 3 independent experiments are shown (** $P < .01$, *** $P < .001$, **** $P < .0001$; 1-way analysis of variance with Dunnett's multiple comparison test). (C) AKT inhibitor-induced cell death in HMCLs can be rescued by FOXO1 inhibition ($n = 5$). HMCLs were treated for 3 days with 3.2 μ M MK2206 AKT inhibitor, with (orange bars) or without (purple bars) 100 nM of the FOXO1 inhibitor AS1842856. Mean \pm SEM of 3 independent experiments are shown (* $P < .05$, ** $P < .01$, *** $P < .001$, **** $P < .0001$; unpaired Student t test with Welch's correction). (D) Cell death of primary MM patient plasma cells induced by AKT inhibitor MK2206 (2.5 μ M) can be overcome by the FOXO1 inhibitor AS1842856 ($n = 5$). Cells were treated for 3 days with 3.2 μ M MK2206 AKT inhibitor, with (orange bars) or without (purple bars) 100 nM of the FOXO1 inhibitor AS1842856. Mean \pm SEM of 3 technical replicates are shown (** $P < .01$, *** $P < .001$, **** $P < .0001$; unpaired Student t test with Welch's correction). Specific cell death in these experiments was determined by 7-AAD viability dye staining and flow cytometry. ns, not significant.

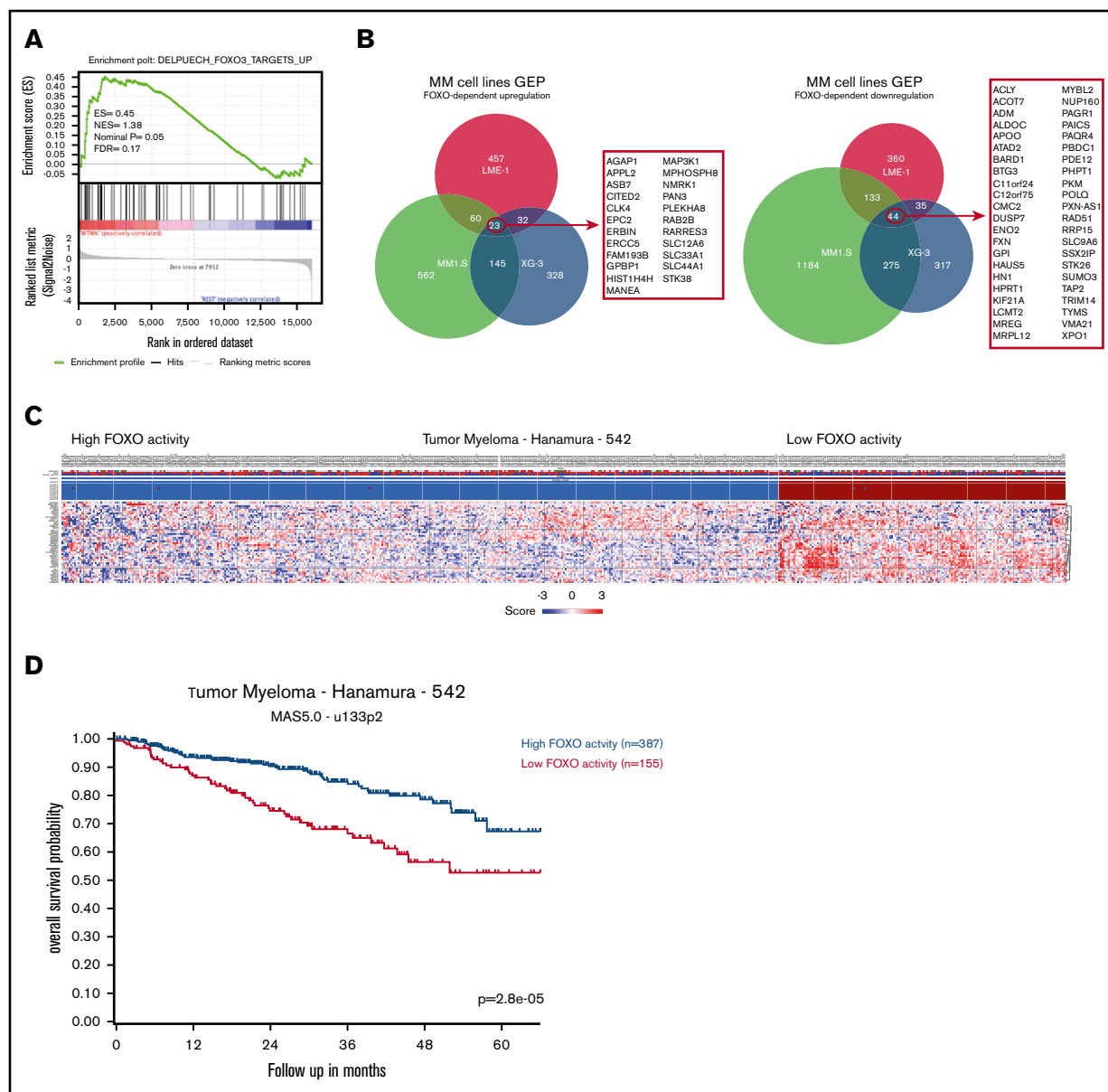


Figure 3. Identification of FOXO-dependent gene signatures in MM cells. Independent LME-1 FOXO1 knockout clones ($n = 2$), MM1.S FOXO3 knockout clones ($n = 2$), and XG-3 FOXO3 knockout clones and their respective control clones ($n = 2$) were treated for 20 hours with 2.5 μM MK2206 AKT inhibitor, or left untreated, and subjected to GEP. (A) GSEA enrichment plot of upregulated FOXO3 target genes (DELPUECH_FOXO3_TARGETS_UP) in WT “cas9 only” (WT) clones treated for 20 hours with 2.5 μM MK2206 (“WTMK”; left side of the plot) vs MK2206-treated FOXO knockout clones, untreated WT, and FOXO knockout clones (“REST”; right side of the plot) from the LME-1, MM1.S, and XG-3 HMCLs combined. False discovery rate (FDR), enrichment score (ES), normalized enrichment score (NES), and P value are indicated in the enrichment plot. (B) Area proportional Venn diagrams depicting the number of genes that are upregulated (left panel) or downregulated (right panel) in a FOXO-dependent fashion upon AKT inhibition. Genes that overlap in all 3 HMCLs are listed alongside the Venn diagrams. Differentially expressed genes between the groups were defined based on P values, using the following cutoffs: LME-1, $P < .15$; MM1.S, $P < .01$; XG-3, $P < .02$ (analysis of variance corrected for multiple testing by FDR). (C) k -means clustering results (10 rounds, 2 groups, blue and red boxes) and z score heat maps based on the genes that are downregulated upon AKT inhibition in a FOXO-dependent fashion and overlapped in all 3 HMCLs (Figure 3B) in a patient GEP dataset. This set contains GEP and survival data of 542 patients with MM. Blue depicts downregulated gene expression, and red depicts upregulated gene expression. (D) Kaplan-Meier plot depicting overall survival of patients with MM from the GEP dataset, using k -means clustering-derived groups representing high and low expression of FOXO target genes.

established direct FOXO targets *CITED2* (found in all 3 HMCLs) and *PIK3CA* (found in LME-1 and XG-3).^{37,38} Despite this overlap, the majority of FOXO-dependent genes were specific for the different HMCLs, underscoring the heterogeneous and context-dependent nature of the transcriptional consequences of FOXO activation.

The FOXO-dependent downregulated genes found in all 3 HMCLs (FOXO_shared_down) were used to perform a k -means unsupervised learning analysis (2 groups, 10 rounds) on a GEP dataset of patients with MM ($n = 542$) that includes clinical data.³⁹ Patients were clustered in 2 groups with, respectively, low expression of

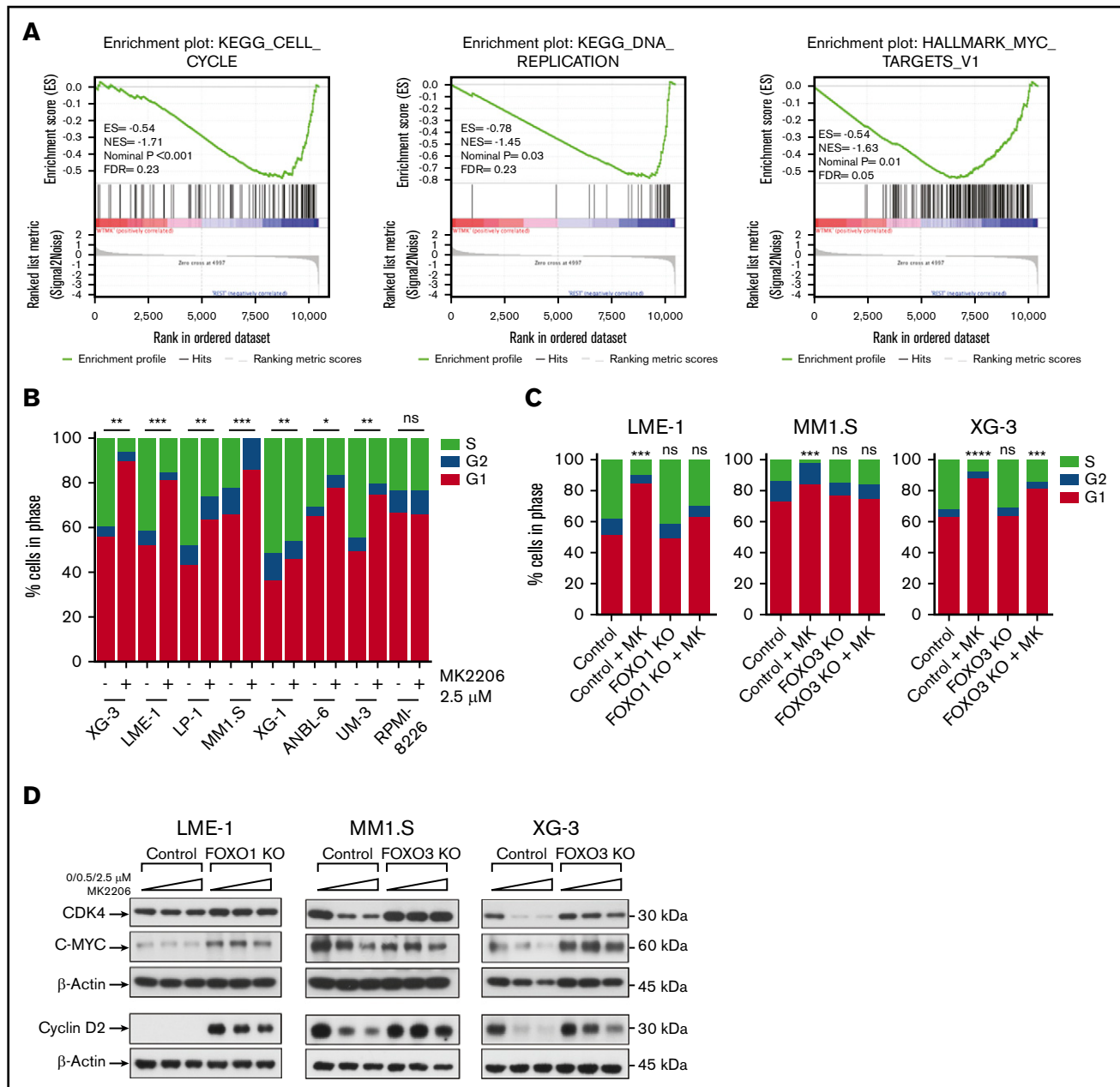


Figure 4. FOXO activation impairs proliferation of MM cells. (A) GSEA enrichment plots show a significant depletion of cell cycle and proliferation-associated gene sets in WT "cas9 only" (WT) clones treated for 20 hours with 2.5 μ M MK2206 ("WTMK"; left side of the plots) vs MK2206-treated FOXO knockout clones and untreated WT and FOXO knockout clones ("REST"; right side of the plots). For GSEA, GEP datasets from the LME-1, MM1.S, and XG-3 HMCLs were combined. False discovery rate (FDR), enrichment score (ES), normalized enrichment score (NES), and *P* values are indicated in the enrichment plots. (B) Bromodeoxyuridine incorporation cell cycle analysis of HMCLs (*n* = 8) treated for 20 hours with 2.5 μ M MK2206. Bromodeoxyuridine incorporation and DNA content were assessed by using flow cytometry. Sub-G1 phase (dead) cells were excluded from the analysis. Percentages of cells in the G1, S, and G2 phases of the cell cycle are depicted. Statistical analysis (1-way analysis of variance with Fisher's least significant difference posttest) was performed on the percentages of cells in S phase (**P* < .05, ***P* < .01, ****P* < .001). The mean values of 3 experiments are depicted. (C) AKT inhibition leads to a FOXO-dependent G1 phase arrest. Cell cycle analysis of LME-1, MM1.S, and XG-3 HMCLs and their respective FOXO1 or FOXO3 knockout clones were treated overnight with 2.5 μ M MK2206 (MK). Percentages of cells in the G1, S, and G2 phases of the cell cycle are depicted. Statistical analysis (1-way analysis of variance with Bonferroni's multiple comparison test) was performed on the percentages of cells in S phase compared with untreated control clones (****P* < .001, *****P* < .0001). The mean values of 3 experiments are depicted. (D) Immunoblot analysis of cell cycle and proliferation-associated proteins in LME-1, MM1.S, and XG-3 control clones and their respective FOXO1 or FOXO3 knockout clones treated overnight with increasing concentrations of 0/0.5/2.5 μ M MK2206. β -actin was used as loading control.

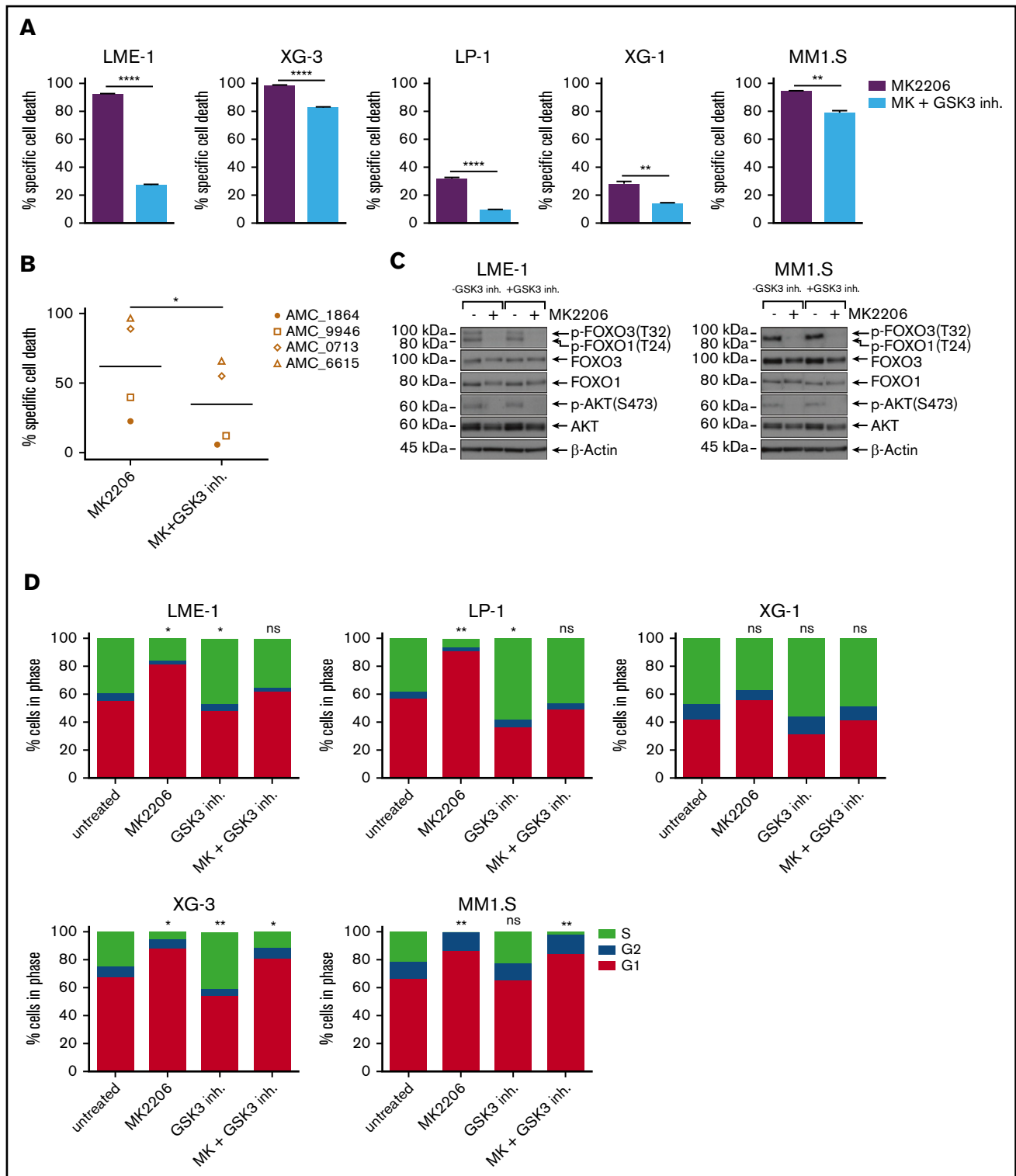


Figure 5. Inhibition of GSK3 partially relieves AKT dependency of MM cells. (A) GSK3 inhibition partially rescued AKT inhibitor–induced cell death in HMCLs ($n = 5$). Cells were cotreated with $3.2 \mu\text{M}$ MK2206 and $1 \mu\text{M}$ GSK3 inhibitor (GSK3 inh.) CHIR99021 for 3 days. Mean \pm SEM of 3 independent experiments are shown ($**P < .01$, $****P < .0001$; unpaired Student t test with Welch's correction). (B) Partial rescue of AKT inhibitor–induced cell death in primary MM patient plasma cells ($n = 4$). Cells were treated for 3 days with $2.5 \mu\text{M}$ MK2206 and $1 \mu\text{M}$ CHIR99021. Specific cell death was calculated based on 7-AAD viability dye staining and flow cytometry. Means of 3 technical replicates are displayed ($*P < .05$; Wilcoxon signed-rank test). (C) Immunoblot analysis of AKT, FOXO1, FOXO3, phospho-AKT-S473, and phospho-Thr24 FOXO1/phospho-Thr32 FOXO3 in LME-1 cells and MM1.S cells treated overnight with $2.5 \mu\text{M}$ MK2206, with or without $1 \mu\text{M}$ CHIR99021. β -actin was used as loading control. (D) Bromodeoxyuridine incorporation cell cycle analysis of HMCLs ($n = 5$) treated overnight with $2.5 \mu\text{M}$ MK2206 and $1 \mu\text{M}$ CHIR99021. Bromodeoxyuridine incorporation and

FOXO-suppressed genes (signifying high FOXO activity) vs high expression of FOXO-suppressed genes (low FOXO activity) (Figure 3C). Importantly, patients with high expression of FOXO-suppressed genes, reflecting high AKT activity, exhibit an inferior overall survival ($P = .000028$) (Figure 3D). The 90% survival was 9 months in this group with low FOXO activity vs 25 months in the high FOXO activity group, and the 2-year survival was 75% vs 91%. These results show that the loss of FOXO activity (and/or increased AKT activity) results in a more aggressive disease course, consistent with a tumor-suppressive role of FOXO in MM.

Activation of FOXO causes cell cycle arrest in HMCLs

Further inspection of the GSEA data on the combined datasets revealed significant depletion of cell cycle and DNA replication/repair-associated gene sets in the MK2206-treated control clones (Figure 4A; supplemental Figure 4A), indicating that activation of FOXO induced cell cycle exit. In agreement, patients with MM clustered according to high FOXO activity showed a significant depletion of these gene sets (supplemental Figure 4B).

Correspondingly, cell cycle analysis showed that abrogation of AKT kinase activity resulted in a significant loss of S phase and a concomitant increase in G1 phase in 7 of 8 HMCLs tested (Figure 4B), including the UM-3 HMCL that does not depend on AKT signaling for survival (Figure 1A). Cell cycle exit required FOXO1 in LME-1 and FOXO3 in MM1.S and XG-3 (Figure 4C). Expression of the cyclin-dependent kinase 4 (CDK4) protein, which regulates G1 phase progression, was decreased in a FOXO3-dependent fashion in MM1.S and XG-3 cells. In contrast, CDK4 remained largely unaffected in LME-1 cells. Protein expression of C-MYC was reduced in all 3 cell lines in a FOXO-dependent manner, which is also reflected in the GSEA analysis of the MYC targets gene set (Figure 4A). Furthermore, C-MYC displayed higher basal protein levels in the FOXO1-deficient LME-1 cells and FOXO3-deficient XG-3 cells compared with control cells. Protein expression of cyclin D2 showed FOXO3-dependent down-modulation in MM1.S and XG-3 but seemed to be activated in the FOXO1-deficient LME-1 cells (Figure 4D). Analysis of GEP data indicated that the levels of *CDK4* messenger RNA (mRNA) were consistently down-modulated by FOXO3 activation in MM1.S and XG-3, whereas the mRNA levels of *CDKN1B* were upregulated by FOXO3 activation. This was not observed in LME-1, suggesting that *CDK4* and *CDKN1B* gene transcription is regulated by FOXO3 but not FOXO1. In contrast, *C-MYC* mRNA levels were not significantly affected in any of the HMCLs (supplemental Figure 5). These data indicate that the effects of FOXO activation on the cell cycle involves both transcriptional and posttranscriptional mechanisms, which are context dependent but nonetheless result in a uniform cell cycle exit.

Activation of GSK3 kinase activity induces cell death and cell cycle arrest in MM cells

GSK3 is an important physiological target of AKT that is inhibited by phosphorylation (Figure 1C-D).¹⁹ Activation of GSK3 downstream

of AKT and PI3K inhibition has been implicated in apoptosis and cell cycle arrest.^{20,40} Correspondingly, the GSK3-specific kinase inhibitor CHIR99021 significantly diminished cell death induced by abrogation of AKT kinase activity in MM cells. Inhibition of GSK3 resulted in a partial rescue of MK2206-induced cell death, ranging from a 1.4-fold decrease in MM1.S cells to a 3.4-fold decrease in LME-1 cells (Figure 5A). A similar range of decrease in AKT inhibitor-induced cell death was observed in primary MM patient plasma cells cotreated with CHIR99021 (Figure 5B). Whereas the AKT inhibitor caused a slight decrease in the total protein levels of AKT, FOXO1, or FOXO3 in MM1.S and LME-1, the GSK3 inhibitor did not affect total protein levels or their phosphorylation status (Figure 5C). GSK3 inhibition prevented AKT inhibitor-induced cell cycle arrest in the LP-1 and LME-1 HMCLs, whereas it had a modest effect in XG-3 and MM1.S. The effects of AKT inhibitor and GSK3 inhibitor treatment in XG-1 displayed a similar trend on the cell cycle as LME-1 and LP-1 but did not reach significance (Figure 5D). Of note, in LME-1, LP-1, and XG-3 cells, a significant increase in S phase was observed upon treatment with the GSK3 inhibitor alone, suggesting that constitutive AKT signaling in these HMCLs does not completely impede GSK3 kinase activity. These results indicate that GSK3 is a tumor suppressor in MM and acts in a cooperative fashion with FOXO TFs.

AKT signaling stabilizes MCL1 protein by inhibiting FOXO- and GSK3-mediated MCL1 turnover

Previously, it was shown that AKT and GSK3 kinase activity are involved in apoptosis by regulating the protein stability of MCL1,^{25,41,42} a BCL2-family member that is essential for the survival of nonmalignant plasma cells and myeloma cells.^{26,43} These findings prompted us to investigate the effects of AKT signaling on MCL1 protein levels in MM. Inhibition of AKT decreased MCL1 protein expression in an FOXO- and GSK3-dependent fashion in the LME-1, MM1.S, and XG-3 HMCLs (Figure 6A). Similarly, AKT inhibition decreased MCL1 protein expression in primary MM cells (Figure 6B). In contrast, *MCL1* mRNA expression increased in an FOXO-dependent manner after AKT inhibition in the LME-1, MM1.S, and XG-3 HMCLs (supplemental Figure 6A), prompting us to investigate the effects of AKT inhibition on MCL1 protein stability. Cycloheximide chase experiments showed that AKT regulates MCL1 protein stability in HMCLs sensitive to AKT inhibition (Figure 6C). In contrast, BCL2 and BCL-XL protein stability remained unchanged under similar conditions in all tested HMCLs (supplemental Figure 6B). In agreement, overexpression of MCL1 in LME-1, MM1.S, and XG-3 obviated the requirement for AKT kinase activity for survival (Figure 6D-E; supplemental Figure 6C). The S63845 small molecule inhibits MCL1 and displays potent antimyeloma activity.⁴⁴ Based on our results, we questioned whether interference with AKT signaling sensitizes myeloma cells for this MCL1 inhibitor. We exposed LME-1, MM1.S, and XG-3 cells, which require AKT pro-survival signaling, and UM-3 and RPMI-8226 cells, which are independent from AKT, to increasing concentrations of MK2206, S63845, and the combination of both. A clear potentiating effect on cell death was observed with the

Figure 5. (continued) DNA content were assessed by using flow cytometry. Sub-G1 phase (dead) cells were excluded from the analysis. Percentages of cells in the G1, S, and G2 phases of the cell cycle are depicted. Statistical analysis (1-way analysis of variance with Bonferroni's multiple comparison test) was performed on the percentages of cells in S phase compared with untreated control cultures. Cultures were performed in triplicate (* $P < .05$, ** $P < .01$).

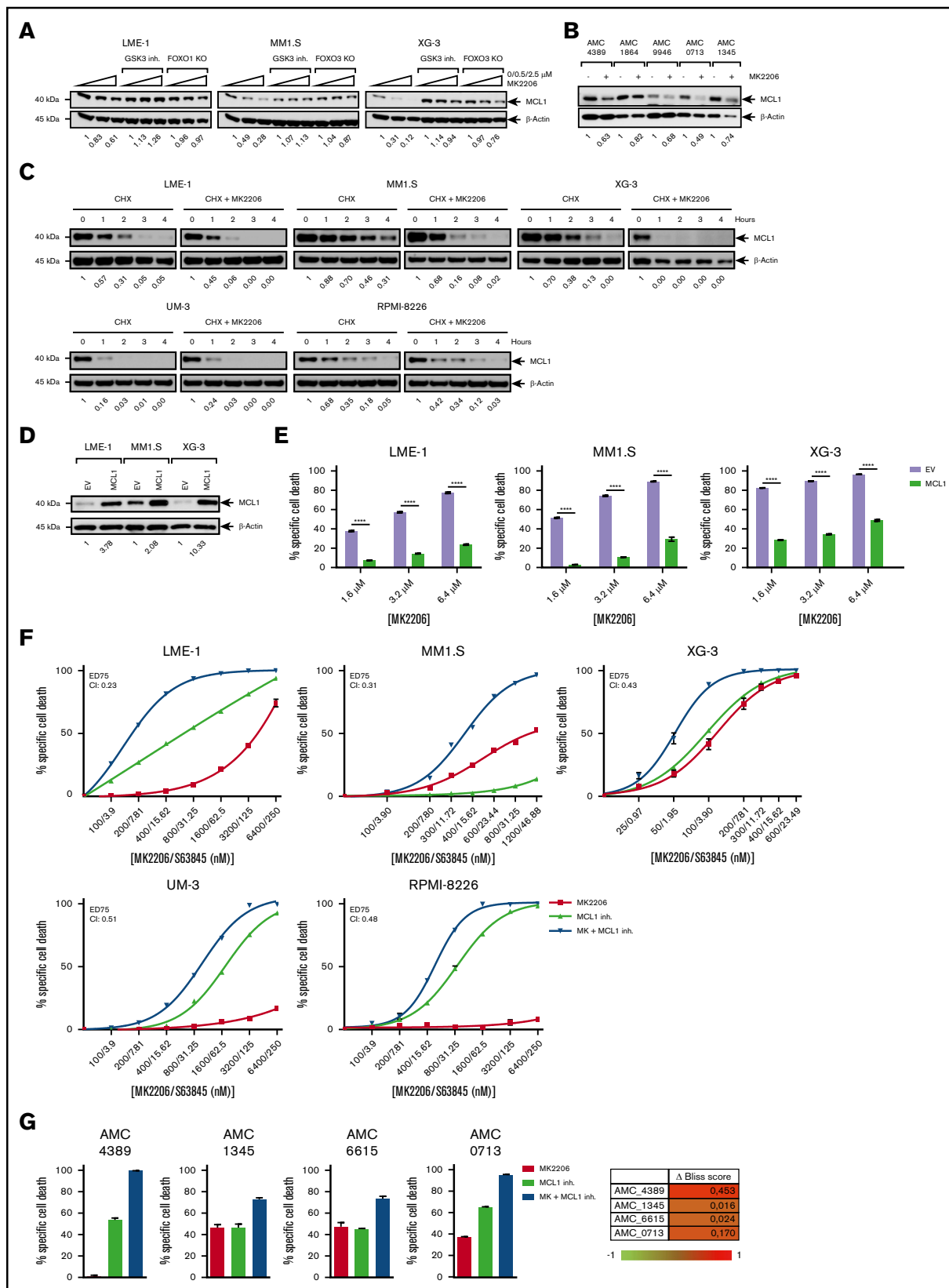


Figure 6. AKT inhibition in MM cells leads to the FOXO/GSK3-mediated MCL1 down-modulation resulting in cell death. (A) Immunoblot analysis of MCL1 protein expression in WT “cas9 only” clones treated overnight with increasing concentrations of MK2206 (0, 0.5, 2.5 μM) with or without 1 μM GSK3 inhibitor (GSK3 inh.) CHIR99021, and in MK2206-treated (0, 0.5, 2.5 μM) FOXO1 or FOXO3 knockout HMCLs. (B) Immunoblot analysis of MCL1 protein expression in primary MM patient plasma

combination of inhibitors, even in the AKT-independent HMCLs (Figure 6F; supplemental Figure 7A).

In accordance with the observed results in HMCLs, the combination of AKT and MCL1 inhibitors resulted in cell death consistently higher than the predicted Bliss score in primary MM cells, indicating a potentiating effect of this drug combination (Figure 6G; supplemental Figure 7B). These results indicate that the FOXO- and GSK3-mediated decrease in MCL1 protein expression after AKT inhibition sensitizes myeloma cells for the MCL1-specific inhibitor S63845, improving the efficacy of these novel therapeutic modalities.

Discussion

Here we showed that the FOXO1 and FOXO3 TFs and the GSK3 kinase act as AKT-repressed tumor suppressors in MM cells. We provide evidence that the prosurvival AKT signaling in MM hinges on the inhibition of FOXO1/3 and GSK3. Importantly, we showed the MM-associated AKT-FOXO axis has clinical implications, as we identified a set of FOXO-repressed target genes that is related to overall survival rates in patients with MM, wherein low FOXO activity (reflecting high AKT activity) classified a patient subgroup with inferior survival.

We showed that suppression of FOXO1/3 and GSK3 by AKT is required for proliferation and survival of MM cells, by regulating the expression of genes involved in cell cycle progression and by regulating the turnover of the antiapoptotic MCL1 protein. We showed that targeting the AKT pathway greatly increased the efficacy of the recently developed MCL1 inhibitor S63845.⁴⁴ These findings could have clinical consequences, as some recent clinical trials that study MCL1 inhibitors were suspended due to reported cardiotoxicity. Our results indicate that the dosing of the MCL1 inhibitor could be drastically reduced when combined with AKT inhibitors, thereby potentially diminishing the risk of these side effects. The simultaneous targeting of AKT and MCL1 can be considered a vertical inhibition strategy, in which 2 points of the same pathway are inhibited. Similar vertical inhibition strategies for the PI3K/AKT/mTOR pathway have shown to be synergistic in multiple cancer types.⁴⁵⁻⁴⁷

The tumor-suppressive roles of FOXO1/3 and GSK3 further explain the constitutive activation of the PI3K/AKT pathway in MM cells, underscoring its crucial function in tumor cell survival. Whether PI3K/AKT signaling has a similar role in the maintenance of normal plasma cells remains unknown. However, AKT activity was shown to

be important in the development of normal plasma cells, as active FOXO1 seemed to inhibit plasma cell formation.^{11,48} The role of FOXO3 in plasma cell differentiation is less clear, as FOXO3-deficient mouse mature B cells show no apparent defects in plasma cell development.¹² However, expression of FOXO3 increases from germinal center B cells to plasma cells.⁴⁹ In agreement with our findings in MM, a report on classical Hodgkin lymphoma showed that FOXO acts as a tumor suppressor.⁵⁰ In contrast, in most mature B-cell malignancies, FOXO seems to drive tumor progression, as FOXO activity is maintained and even enforced through activating mutations.⁴⁸ These observations suggest that FOXO transcription factors act in a context-dependent fashion in normal and malignant plasma cells. This is emphasized by our GEP data, showing relatively limited overlap between FOXO-regulated genes in 3 different HMCLs. Despite this apparent heterogeneity, the effects of FOXO activation on proliferation and cell death were remarkably uniform, as reflected by gene expression enrichment analysis performed on the combined datasets. There are some reports that suggest that FOXO1 and FOXO3 are functionally linked and act redundantly, for instance in autophagy⁵¹ and development of thymic lymphomas and hemangiomas,⁵² whereas in lymphocyte development, these FOXO transcription factors have specialized as well as redundant functions.^{11,12} However, in MM cells, the functions of FOXO1 and FOXO3 suggest there is no obvious overlap, as the loss of FOXO1 was not compensated by FOXO3, or vice versa, despite increased expression of the alternate family member (supplemental Figure 2C-D).

A major difference between normal and malignant plasma cells is their proliferative capacity, which can be attributed to recurrent genomic abnormalities that result in the aberrant expression of cell cycle-related genes, such as D-type cyclins and C-MYC, which are nearly universal events in MM.⁵³ Despite aberrant expression, these cell cycle-associated genes nevertheless require AKT signaling as these are repressed by FOXO1/3 upon AKT inhibition, indicating that the AKT pathway is an integral part of the oncogenic proliferative program of MM cells. AKT signaling is required to inhibit a FOXO-dependent G1 phase arrest in MM cells, consistent with earlier reports on lymphomas and other cancer cell types.⁵⁴⁻⁵⁷ As previously shown, FOXO may cause cell cycle arrest by driving the expression of the cyclin-dependent kinase inhibitor p27(kip1),⁵⁸ and by reducing the expression of D-type cyclins.⁵⁹ In agreement, we observed FOXO-dependent down-modulation of cyclin D2. Furthermore, CDK4 and C-MYC protein expression was also downregulated in a FOXO-dependent fashion, whereas p27(kip1)

Figure 6. (continued) cells (n = 5) treated overnight with or without 2.5 μ M MK2206. (C) Immunoblot analysis of MCL1 protein stability in HMCLs (n = 5) after cycloheximide (CHX) treatment (200 μ g/mL), with or without pretreatment of 2.5 μ M MK2206 for 12 hours. Cells were treated with CHX as indicated by depicted time points. (D) Immunoblot analysis of MCL1 protein expression in HMCLs (n = 3) overexpressing MCL1. HMCLs expressing empty vector (EV) were used as controls. β -actin was used as loading control. (E) MCL1 overexpression rescues AKT inhibitor-induced cell death. HMCLs overexpressing MCL1 (n = 3) were cultured for 3 days with various concentrations of MK2206 (1.6, 3.2, 6.4 μ M). HMCLs transfected with EV were used as controls. Specific cell death was assessed by 7-AAD viability dye staining and flow cytometry. Mean \pm SEM of 3 independent experiments are shown (**** P < .0001; 1-way analysis of variance with Bonferroni's multiple comparison test). (F) Inhibition of AKT sensitizes HMCLs (n = 5) to MCL1 inhibitor-induced cell death. Cells were treated for 3 days with various concentrations of MK2206 and MCL1 inhibitor (MCL1 inh.) S63845, as indicated on the x-axis of the graphs. Percentages of specific cell death are depicted. Mean \pm SEM values of 3 experiments are shown. Chou-Talalay combination index (CI) values at ED75 (effective dose causing 75% cell death) are indicated in the graphs. (G) Inhibition of AKT potentiates for MCL1 inhibitor-induced cell death in primary patient plasma cells (n = 4). Cells were treated for 3 days with a concentration of MK2206 and S63845 (2.5 μ M MK2206, 100 nM S63845 for AMC_4389, 100 nM MK2206, 4 nM S63845 for AMC_1345 and AMC_6615, and 500 nM MK2206, 20 nM S63845 for AMC_0713) either as single drug or a combination. Mean \pm SEM values of 3 technical replicates are shown. The Δ Bliss score was calculated by subtracting the predicted cell death (Bliss) from the actual observed effect of the combined inhibitors; -1 indicates an antagonistic effect and +1 indicates a synergistic effect.

seemed to be upregulated, and in this way impinges on CDK4, as p27(kip1) is known to bind and inactivate CDK4. In agreement, GSEA indicated that the expression of MYC target genes required AKT signaling (supplemental Figure 4). In addition, DNA repair gene expression signatures were significantly down-modulated upon activation of FOXO1/3 in MM, suggesting that the combination of AKT inhibitors with DNA-damaging agents might be a promising treatment option for patients with MM.

Interestingly, AKT-mediated phosphorylation of FOXO1 or FOXO3 was not affected by GSK3 kinase inhibition, suggesting that GSK3 did not act upstream of FOXO1/3. These data indicate that FOXO1/3 and GSK3 act in a cooperative fashion. The role of GSK3 in the regulation of cell death downstream of PI3K/AKT signaling was described previously in various types of cancer.^{20,60-63} However, the role of GSK3 in MM is less clear, as both pro-survival and proapoptotic functions have been ascribed to this kinase.⁶⁴⁻⁷⁰ To our knowledge, our results are the first to indicate that GSK3 is an important mediator of cell death in MM cells controlled by AKT signaling. The partial and heterogeneous effects of GSK3 inhibition likely reflects the molecular heterogeneity of the HMCLs and patient samples used in this study.

Taken together, our data provide crucial insights into the AKT signaling dependence of MM cells, revealing that the constitutive AKT activity in MM masks important tumor cell vulnerabilities that may be exploited therapeutically; for example, by combination therapies aimed at the activation of FOXO and the inhibition of downstream targets.

References

1. Palumbo A, Anderson K. Multiple myeloma. *N Engl J Med*. 2011;364(11):1046-1060.
2. Tu Y, Gardner A, Lichtenstein A. The phosphatidylinositol 3-kinase/AKT kinase pathway in multiple myeloma plasma cells: roles in cytokine-dependent survival and proliferative responses. *Cancer Res*. 2000;60(23):6763-6770.
3. Hsu J, Shi Y, Krajewski S, et al. The AKT kinase is activated in multiple myeloma tumor cells. *Blood*. 2001;98(9):2853-2855.
4. Hideshima T, Nakamura N, Chauhan D, Anderson KC. Biologic sequelae of interleukin-6 induced PI3-K/Akt signaling in multiple myeloma. *Oncogene*. 2001;20(42):5991-6000.
5. Lentzsch S, Chatterjee M, Gries M, et al. PI3-K/AKT/FKHR and MAPK signaling cascades are redundantly stimulated by a variety of cytokines and contribute independently to proliferation and survival of multiple myeloma cells. *Leukemia*. 2004;18(11):1883-1890.
6. Hyun T, Yam A, Pece S, et al. Loss of PTEN expression leading to high Akt activation in human multiple myelomas. *Blood*. 2000;96(10):3560-3568.
7. Chang H, Qi XY, Claudio J, Zhuang L, Patterson B, Stewart AK. Analysis of PTEN deletions and mutations in multiple myeloma. *Leuk Res*. 2006;30(3):262-265.
8. Manning BD, Toker A. AKT/PKB signaling: navigating the network. *Cell*. 2017;169(3):381-405.
9. Hornsveid M, Dansen TB, Derksen PW, Burgering BMT. Re-evaluating the role of FOXOs in cancer. *Semin Cancer Biol*. 2018;50:90-100.
10. Herzog S, Hug E, Meixlsperger S, et al. SLP-65 regulates immunoglobulin light chain gene recombination through the PI(3)K-PKB-Foxo pathway. *Nat Immunol*. 2008;9(6):623-631.
11. Dengler HS, Baracho GV, Omori SA, et al. Distinct functions for the transcription factor Foxo1 at various stages of B cell differentiation. *Nat Immunol*. 2008;9(12):1388-1398.
12. Hinman RM, Nichols WA, Diaz TM, Gallardo TD, Castrillon DH, Satterthwaite AB. Foxo3^{-/-} mice demonstrate reduced numbers of pre-B and recirculating B cells but normal splenic B cell sub-population distribution. *Int Immunol*. 2009;21(7):831-842.
13. Chen J, Limon JJ, Blanc C, Peng SL, Fruman DA. Foxo1 regulates marginal zone B-cell development. *Eur J Immunol*. 2010;40(7):1890-1896.
14. Ochodnicka-Mackovicova K, Bahjat M, Bloedjes TA, et al. NF- κ B and AKT signaling prevent DNA damage in transformed pre-B cells by suppressing RAG1/2 expression and activity. *Blood*. 2015;126(11):1324-1335.
15. Dominguez-Sola D, Kung J, Holmes AB, et al. The FOXO1 transcription factor instructs the germinal center dark zone program. *Immunity*. 2015;43(6):1064-1074.

Acknowledgments

This research was supported by The Netherlands Organization for Scientific Research Innovative Research Incentives Scheme (VIDI grant no.16126355) and by grant AMC 2018-11597 of the Dutch Cancer Society (both J.E.J.G.)

Authorship

Contribution: J.E.J.G. and T.A.B. designed the research; T.A.B., G.d.W., C.M., and J.E.J.G. performed the experiments; E.E., R.J.B., C.J.M.v.N., S.T.P., M.S., and J.E.J.G. analyzed the data; T.A.B., G.d.W., and J.E.J.G. wrote the manuscript; and all authors edited the manuscript.

Conflict-of-interest disclosure: E.E. received research funding from Hoffmann–La Roche Ltd. and from Gilead Sciences Inc. The remaining authors declare no competing financial interests.

ORCID profiles: T.A.B., 0000-0002-7279-0182; G.d.W., 0000-0002-0928-9977; C.M., 0000-0003-3031-2294; E.E., 0000-0003-0561-6640; R.J.B., 0000-0002-5173-3138; C.J.M.v.N., 0000-0001-7907-7390; M.S., 0000-0002-3135-5109; J.E.J.G., 0000-0001-6894-3441.

Correspondence: Jeroen E. J. Guikema, Department of Pathology, Amsterdam UMC, University of Amsterdam, Meibergdreef 9, 1105 AZ Amsterdam, The Netherlands; e-mail: j.e.guikema@amsterdamumc.nl.

16. Sander S, Chu VT, Yasuda T, et al. PI3 kinase and FOXO1 transcription factor activity differentially control B cells in the germinal center light and dark zones. *Immunity*. 2015;43(6):1075-1086.
17. Calnan DR, Brunet A. The FoxO code. *Oncogene*. 2008;27(16):2276-2288.
18. van der Vos KE, Coffey PJ. FOXO-binding partners: it takes two to tango. *Oncogene*. 2008;27(16):2289-2299.
19. Cross DA, Alessi DR, Cohen P, Andjelkovich M, Hemmings BA. Inhibition of glycogen synthase kinase-3 by insulin mediated by protein kinase B. *Nature*. 1995;378(6559):785-789.
20. Pap M, Cooper GM. Role of glycogen synthase kinase-3 in the phosphatidylinositol 3-Kinase/Akt cell survival pathway. *J Biol Chem*. 1998;273(32):19929-19932.
21. Fang X, Yu SX, Lu Y, Bast RC Jr., Woodgett JR, Mills GB. Phosphorylation and inactivation of glycogen synthase kinase 3 by protein kinase A. *Proc Natl Acad Sci U S A*. 2000;97(22):11960-11965.
22. Schubert F, Rapp J, Brauns-Schubert P, et al. Requirement of GSK-3 for PUMA induction upon loss of pro-survival PI3K signaling. *Cell Death Dis*. 2018;9(5):470.
23. Cohen P, Frame S. The renaissance of GSK3. *Nat Rev Mol Cell Biol*. 2001;2(10):769-776.
24. Linseman DA, Butts BD, Precht TA, et al. Glycogen synthase kinase-3beta phosphorylates Bax and promotes its mitochondrial localization during neuronal apoptosis. *J Neurosci*. 2004;24(44):9993-10002.
25. Maurer U, Charvet C, Wagman AS, Dejardin E, Green DR. Glycogen synthase kinase-3 regulates mitochondrial outer membrane permeabilization and apoptosis by destabilization of MCL-1. *Mol Cell*. 2006;21(6):749-760.
26. Peperzak V, Vikström I, Walker J, et al. Mcl-1 is essential for the survival of plasma cells [published correction appears in *Nat Immunol*. 2013;14(8):877]. *Nat Immunol*. 2013;14(3):290-297.
27. Wuillème-Toumi S, Robillard N, Gomez P, et al. Mcl-1 is overexpressed in multiple myeloma and associated with relapse and shorter survival. *Leukemia*. 2005;19(7):1248-1252.
28. van Andel H, Ren Z, Koopmans I, et al. Aberrantly expressed LGR4 empowers Wnt signaling in multiple myeloma by hijacking osteoblast-derived R-spondins. *Proc Natl Acad Sci U S A*. 2017;114(2):376-381.
29. Ochodnicka-Mackovicova K, Bahjat M, Maas C, et al. The DNA damage response regulates RAG1/2 expression in pre-B cells through ATM-FOXO1 signaling. *J Immunol*. 2016;197(7):2918-2929.
30. Schneider CA, Rasband WS, Eliceiri KW. NIH Image to ImageJ: 25 years of image analysis. *Nat Methods*. 2012;9(7):671-675.
31. Hulsen T, de Vlieg J, Alkema W. BioVenn—a web application for the comparison and visualization of biological lists using area-proportional Venn diagrams. *BMC Genomics*. 2008;9(1):488.
32. Subramanian A, Tamayo P, Mootha VK, et al. Gene set enrichment analysis: a knowledge-based approach for interpreting genome-wide expression profiles. *Proc Natl Acad Sci U S A*. 2005;102(43):15545-15550.
33. Jak M, van, Bochove GG, Reits EA, et al. CD40 stimulation sensitizes CLL cells to lysosomal cell death induction by type II anti-CD20 monoclonal antibody GA101. *Blood*. 2011;118(19):5178-5188.
34. Chou T-C. Drug combination studies and their synergy quantification using the Chou-Talalay method. *Cancer Res*. 2010;70(2):440-446.
35. Bliss CI. The toxicity of poisons applied jointly. *Ann Appl Biol*. 1939;26(3):585-615.
36. Nagashima T, Shigematsu N, Maruki R, et al. Discovery of novel forkhead box O1 inhibitors for treating type 2 diabetes: improvement of fasting glycemia in diabetic db/db mice. *Mol Pharmacol*. 2010;78(5):961-970.
37. Bakker WJ, Harris IS, Mak TW. FOXO3a is activated in response to hypoxic stress and inhibits HIF1-induced apoptosis via regulation of CITED2. *Mol Cell*. 2007;28(6):941-953.
38. Hui RC-Y, Gomes AR, Constantinidou D, et al. The forkhead transcription factor FOXO3a increases phosphoinositide-3 kinase/Akt activity in drug-resistant leukemic cells through induction of PIK3CA expression. *Mol Cell Biol*. 2008;28(19):5886-5898.
39. Hanamura I, Huang Y, Zhan F, Barlogie B, Shaughnessy J. Prognostic value of cyclin D2 mRNA expression in newly diagnosed multiple myeloma treated with high-dose chemotherapy and tandem autologous stem cell transplantations. *Leukemia*. 2006;20(7):1288-1290.
40. Diehl JA, Cheng M, Roussel MF, Sherr CJ. Glycogen synthase kinase-3beta regulates cyclin D1 proteolysis and subcellular localization. *Genes Dev*. 1998;12(22):3499-3511.
41. Zhao Y, Altman BJ, Coloff JL, et al. Glycogen synthase kinase 3alpha and 3beta mediate a glucose-sensitive antiapoptotic signaling pathway to stabilize Mcl-1. *Mol Cell Biol*. 2007;27(12):4328-4339.
42. Coloff JL, Macintyre AN, Nichols AG, et al. Akt-dependent glucose metabolism promotes Mcl-1 synthesis to maintain cell survival and resistance to Bcl-2 inhibition. *Cancer Res*. 2011;71(15):5204-5213.
43. Jourdan M, Veyrune JL, De Vos J, Redal N, Couderc G, Klein B. A major role for Mcl-1 antiapoptotic protein in the IL-6-induced survival of human myeloma cells. *Oncogene*. 2003;22(19):2950-2959.
44. Kotschy A, Szlavik Z, Murray J, et al. The MCL1 inhibitor S63845 is tolerable and effective in diverse cancer models. *Nature*. 2016;538(7626):477-482.
45. Ou DL, Lee BS, Lin LI, et al. Vertical blockade of the IGF1R-PI3K/Akt/mTOR pathway for the treatment of hepatocellular carcinoma: the role of survivin. *Mol Cancer*. 2014;13(1):2.
46. Yang S, Xiao X, Meng X, Leslie KK. A mechanism for synergy with combined mTOR and PI3 kinase inhibitors. *PLoS One*. 2011;6(10):e26343.

47. Woo SU, Sangai T, Akcakanat A, Chen H, Wei C, Meric-Bernstam F. Vertical inhibition of the PI3K/Akt/mTOR pathway is synergistic in breast cancer. *Oncogenesis*. 2017;6(10):e385.
48. Ushmorov A, Wirth T. FOXO in B-cell lymphopoiesis and B cell neoplasia. *Semin Cancer Biol*. 2018;50:132-141.
49. Osswald CD, Xie L, Guan H, et al. Fine-tuning of FOXO3A in cHL as a survival mechanism and a hallmark of abortive plasma cell differentiation. *Blood*. 2018;131(14):1556-1567.
50. Vogel MJ, Xie L, Guan H, et al. FOXO1 repression contributes to block of plasma cell differentiation in classical Hodgkin lymphoma. *Blood*. 2014;124(20):3118-3129.
51. Zhou J, Liao W, Yang J, et al. FOXO3 induces FOXO1-dependent autophagy by activating the AKT1 signaling pathway. *Autophagy*. 2012;8(12):1712-1723.
52. Paik JH, Kollipara R, Chu G, et al. FoxOs are lineage-restricted redundant tumor suppressors and regulate endothelial cell homeostasis. *Cell*. 2007;128(2):309-323.
53. Kuehl WM, Bergsagel PL. Molecular pathogenesis of multiple myeloma and its premalignant precursor. *J Clin Invest*. 2012;122(10):3456-3463.
54. Rassidakis GZ, Feretzaki M, Atwell C, et al. Inhibition of Akt increases p27Kip1 levels and induces cell cycle arrest in anaplastic large cell lymphoma. *Blood*. 2005;105(2):827-829.
55. Georgakis GV, Li Y, Rassidakis GZ, Medeiros LJ, Mills GB, Younes A. Inhibition of the phosphatidylinositol-3 kinase/Akt promotes G1 cell cycle arrest and apoptosis in Hodgkin lymphoma. *Br J Haematol*. 2006;132(4):503-511.
56. Rudelius M, Pittaluga S, Nishizuka S, et al. Constitutive activation of Akt contributes to the pathogenesis and survival of mantle cell lymphoma. *Blood*. 2006;108(5):1668-1676.
57. Fekete M, Santiskulvong C, Eng C, Dorigo O. Effect of PI3K/Akt pathway inhibition-mediated G1 arrest on chemosensitization in ovarian cancer cells. *Anticancer Res*. 2012;32(2):445-452.
58. Medema RH, Kops GJ, Bos JL, Burgering BM. AFX-like Forkhead transcription factors mediate cell-cycle regulation by Ras and PKB through p27kip1. *Nature*. 2000;404(6779):782-787.
59. Schmidt M, Fernandez de Mattos S, van der Horst A, et al. Cell cycle inhibition by FoxO forkhead transcription factors involves downregulation of cyclin D. *Mol Cell Biol*. 2002;22(22):7842-7852.
60. Chen XL, Ren KH, He HW, Shao RG. Involvement of PI3K/AKT/GSK3beta pathway in tetrandrine-induced G1 arrest and apoptosis. *Cancer Biol Ther*. 2008;7(7):1073-1078.
61. McDonnell SRP, Hwang SR, Basrur V, et al. NPM-ALK signals through glycogen synthase kinase 3 β to promote oncogenesis. *Oncogene*. 2012;31(32):3733-3740.
62. Rahmani M, Aust MM, Attkisson E, Williams DC Jr., Ferreira-Gonzalez A, Grant S. Dual inhibition of Bcl-2 and Bcl-xL strikingly enhances PI3K inhibition-induced apoptosis in human myeloid leukemia cells through a GSK3- and Bim-dependent mechanism. *Cancer Res*. 2013;73(4):1340-1351.
63. Wang R, Xia L, Gabrilove J, Waxman S, Jing Y. Sorafenib inhibition of Mcl-1 accelerates ATRA-induced apoptosis in differentiation-responsive AML cells. *Clin Cancer Res*. 2016;22(5):1211-1221.
64. G-Amlak M, Uddin S, Mahmud D, et al. Regulation of myeloma cell growth through Akt/Gsk3/forkhead signaling pathway. *Biochem Biophys Res Commun*. 2002;297(4):760-764.
65. Santo L, Vallet S, Hideshima T, et al. AT7519, A novel small molecule multi-cyclin-dependent kinase inhibitor, induces apoptosis in multiple myeloma via GSK-3beta activation and RNA polymerase II inhibition. *Oncogene*. 2010;29(16):2325-2336.
66. Busino L, Millman SE, Scotto L, et al. Fbxw7 α - and GSK3-mediated degradation of p100 is a pro-survival mechanism in multiple myeloma. *Nat Cell Biol*. 2012;14(4):375-385.
67. Piazza F, Manni S, Tubi LQ, et al. Glycogen synthase kinase-3 regulates multiple myeloma cell growth and bortezomib-induced cell death. *BMC Cancer*. 2010;10(1):526.
68. Nekova TS, Dotterweich J, Schütze N, Einsele H, Stuhler G. Small molecule enhancers of rapamycin induce apoptosis in myeloma cells via GSK3A/B preferentially within a protective bone marrow microenvironment. *Br J Haematol*. 2014;167(2):272-274.
69. Herath NI, Rocques N, Garancher A, Eychène A, Pouponnot C. GSK3-mediated MAF phosphorylation in multiple myeloma as a potential therapeutic target. *Blood Cancer J*. 2014;4(1):e175.
70. Qiang YW, Ye S, Chen Y, et al. MAF protein mediates innate resistance to proteasome inhibition therapy in multiple myeloma. *Blood*. 2016;128(25):2919-2930.